Appl Microbiol Biotechnol (2013) 97:10373–10380
DOI 10.1007/s00253-013-4806-0

BIOTECHNOLOGICALLY RELEVANT ENZYMES AND PROTEINS

Interaction between DAHP synthase and chorismate mutase endows new regulation on DAHP synthase activity in *Corynebacterium glutamicum*

Pan-Pan Li · De-Feng Li · Di Liu · Yi-Ming Liu · Chang Liu · Shuang-Jiang Liu

Received: 3 January 2013 / Revised: 19 February 2013 / Accepted: 20 February 2013 / Published online: 7 March 2013

Abstract Previous research on *Corynebacterium glutamicum* revealed that 3-deoxy-D-arabino-heptulosonate 7-phosphate synthase (DS_{Cg}, formerly DS2098) interacts with chorismate mutase (CM_{Cg}, formerly CM0819). In this study, we investigated the interaction by means of structure-guided mutation and enzymatic assays. Our results show that the interaction imparted a new mechanism for regulation of DAHP activity: In the absence of CM_{Cg}, DS_{Cg} activity was not regulated by prephenate, whereas in the presence of CM_{Cg}, prephenate markedly inhibited DS_{Cg} activity. Prephenate competed with the substrate phosphoenolpyruvate, and the inhibition constant (K_i) was determined to be 0.945 mM. Modeling based on the structure of the complex formed between DAHP synthase and chorismate mutase of *Mycobacterium tuberculosis* predicted the interaction surfaces of the putative DS_{Cg}-CM_{Cg} complex. The amino acid residues and structural domains that contributed to the interaction surfaces were experimentally identified to be the ^{212}SPAGARYE^{219} sequence of DS_{Cg} and the ^{60}SGGTR^{64} loop and C-terminus (^{97}RGKLG^{101}) of CM_{Cg}.

Keywords 3-deoxy-D-arabino-heptulosonate 7-phosphate (DAHP) synthase · Chorismate mutase (CM) · Regulation · Shikimate pathway · *Corynebacterium glutamicum*

P.-P. Li · Y.-M. Liu · C. Liu · S.-J. Liu
State Key Laboratory of Microbial Resources,
Institute of Microbiology, Chinese Academy of Sciences,
Beijing 100101, People's Republic of China

D.-F. Li
Institute of Biophysics, Chinese Academy of Sciences,
Beijing 100101, People's Republic of China

D. Liu
Network Information Center, Institute of Microbiology,
Chinese Academy of Sciences,
Beijing 100101, People's Republic of China

Y.-M. Liu · S.-J. Liu (✉)
Environmental Microbiology and Biotechnology Research Center,
Institute of Microbiology, Chinese Academy of Sciences,
Beichen West Road No. 1, Chaoyang District,
Beijing 100101, People's Republic of China
e-mail: liusj@im.ac.cn

Introduction

3-Deoxy-D-arabino-heptulosonate 7-phosphate (DAHP) synthases (DSs; EC 2.5.1.54) catalyze the condensation of phosphoenolpyruvate (PEP) and erythrose 4-phosphate to form DAHP in bacteria, fungi, and plants (Herrmann 1995; Pittard 1996; Romero et al. 1995). Because DSs catalyze the first step of the shikimate pathway (Herrmann 1995), they are tightly regulated by a variety of mechanisms. *Escherichia coli* have three DSs that are sensitive to feedback regulation by phenylalanine (Phe), tryptophan (Trp), or tyrosine (Tyr), respectively (Kikuchi et al. 1997; Romero et al. 1995). *Corynebacterium glutamicum* has two DSs, NCgl0950 DS and NCgl2098; the former is sensitive to feedback inhibition by Tyr and, to a much lesser extent, by Phe and Trp, whereas the latter (hereafter designated DS_{Cg}), is slightly sensitive to feedback inhibition by Trp but is insensitive to Tyr and Phe (Liao et al. 2001; Liu et al. 2008). *Bacillus subtilis* possesses only one DS, which is insensitive to Phe, Tyr, and Trp, but is regulated by the

shikimate pathway intermediates prephenate and chorismate (Wu et al. 2005). Recently, the DS from *Mycobacterium tuberculosis* (DS_{Mt}) has been shown to be subject to unique allosteric regulation: DS_{Mt} is not sensitive to any single aromatic amino acid, but a combination of Trp and Phe significantly inhibits its activity (Webby et al. 2010). More recently, dynamic cross talk between remote binding sites of catalytic products has been identified as the molecular basis for the allosteric regulation (Jiao et al. 2012).

DS_{Mt} plays a key role in the activation and feedback regulation of the branch-point enzyme chorismate mutase from *M. tuberculosis* (CM_{Mt}) (Schneider et al. 2008). Interestingly, DS_{Mt} forms a complex with CM_{Mt}, and complex formation leads to substantial enhancement and synergistic regulation of CM activity by Phe and Tyr in *M. tuberculosis* (Sasso et al. 2009). In contrast, we previously found that in *C. glutamicum*, DS_{Cg} activity is significantly enhanced by chorismate mutase (CM_{Cg}), whereas no enhancement of CM_{Cg} activity by DS_{Cg} is observed (Li et al. 2009), even though DS_{Cg} and CM_{Cg} show 77 and 57 % sequence identities to DS_{Mt} and CM_{Mt}, respectively.

In this study, we investigated the interaction between DS_{Cg} and CM_{Cg}. Structure modeling predicted that DS_{Cg} and CM_{Cg} should form a complex similar to the DS_{Mt}-CM_{Mt} complex (Sasso et al. 2009). In the presence of CM_{Cg}, we found that the DS_{Cg} activity was regulated by prephenate, whereas in the absence of CM_{Cg}, no such regulation was observed. The amino acid residues that contributed to the interaction interfaces of the putative DS_{Cg}-CM_{Cg} complex were identified by means of site-directed mutagenesis and deletion.

Materials and methods

Bacterial strains, plasmids, and cultivation

The bacterial strains and plasmids used in this study are listed in Table 1. *E. coli* strains were grown aerobically on a rotary shaker (150 rpm) at 37 °C in Luria-Bertani (LB) broth or on LB agar [1.5 % (wt/vol)] plates. *C. glutamicum* strains were routinely grown at 30 °C in LB broth on a rotary shaker (150 rpm). Kanamycin and ampicillin were used at concentrations of 50 and 100 $\mu g \times ml^{-1}$, respectively.

Sequence and structure analyses

The sequences of the *M. tuberculosis* and *C. glutamicum* DSs and CMs were retrieved from GenBank (accession nos. 000962 and 003450). Protein sequence alignments and analyses were carried out using the BLAST tool on the NCBI website (http://www.ncbi.nlm.nih.gov) and the ClustalW multiple sequence alignment program (Thompson et al. 1997). The structures of DS_{Mt} and the DS_{Mt}-CM_{Mt} complex were obtained from the Protein Data Bank (PDB: 2B7O; PDB: 2W1A). The protein structure and prephenate docking were analyzed by means of the PyMOL program (Delano 2002) and Ligand Explorer (http://www.pdb.org/pdb/home/home.do).

DNA extraction and manipulation

The total genomic DNA of *C. glutamicum* was isolated according to the procedure of Tauch et al. (Tauch et al. 1995). DNA restriction enzyme digestion, plasmid isolation, and agarose gel electrophoresis were carried out as described by Samsbrook et al. (1989). *E. coli* strains were transformed by electroporation according to the method of Tauch et al. (2002).

PCR amplification of DNA fragments and construction of plasmids

PCR reactions were performed with *Pfu* DNA polymerase (TransGen, Beijing, China). PCR products were purified with an agarose gel DNA fragment recovery kit (Tiangen, Beijing, China). Plasmids pET21-DS_{Cg}, pET28-CM_{Cg}M1, and pET28-CM_{Cg}M2 (Table 1) for expression of wild type and mutant DS_{Cg} and CM_{Cg} in *E. coli* cells were constructed. Primers used for amplification of the entire target genes or DNA fragments are listed in Table 1.

QuikChange site-directed mutagenesis

The plasmids for expression of site-directed mutant proteins DS_{Cg}M1, DS_{Cg}M2, CM_{Cg}M3, and CM_{Cg}M4 were constructed as described by Wang et al. (2008). PCR reactions were performed with *Pfu* DNA polymerase. Reaction mixtures without primers were run in parallel and used as controls. *Dpn*I was added to PCR products to digest the template plasmids; after 3 h at 37 °C, the mixture was transformed into *E. coli* XL1-Blue by electroporation for replication of target plasmids. Primers used for site-directed mutagenesis are listed in Table 1.

Heterologous expression of wild type and mutant DS_{Cg} and CM_{Cg} in *E. coli* cells, preparation of cellular lysates, and protein purification

Plasmids pET28-CM_{Cg}, pET28-CM_{Cg}M1, pET28-CM_{Cg}M2, pET28-CM_{Cg}M3, pET28-CM_{Cg}M4, pET21-DS_{Cg}, pET21-DS_{Cg}M1, and pET21-DS_{Cg}M2 were transformed into *E. coli* BL21 (DE3) by electroporation for heterologous expression of the wild-type and mutated DS and CM genes. Recombinant protein synthesis in *E. coli* BL21 (DE3) cells was initiated by the addition of 0.2 mM isopropyl β-D-1-thiogalactopyranoside, and the mixtures were cultured for 3 h at 30 °C.

Table 1 Bacterial strains, plasmids, and primers used in this study

cc	Relevant characteristic/sequence	Source/reference/note
Strain		
E. coli		
XL1-Blue	*supE*44 *hsdR*17 *recA*1 *endA*1 *gyrA*46 *thi relA*1 *lac*- F′[*proAB*+*lacI*q *lacZ*ΔM15 Tn*10*(tet^T)]	Stratagene (Cat. no. 200249)
BL21 (DE3)	*hsdS gal* (λ*c*I*ts*857 *ind-l Sam7 nin-5 lacUV5*-T7 *gene 1)*	Novagen (Cat. no. 69450-3)
C. glutamicum		
RES167	Restriction-deficient mutant of ATCC13032, Δ (*cglIM-cglIR-cglIIR*)	From University of Bielefeld
Plasmid		
pET28a	Expression vector with N-terminal hexahistidine affinity tag	Novagen
pET28-CM_{Cg}	pET28a derivative for expression of CM_{Cg}	(Li et al. 2009)
pET28-CM_{Cg}M1	Expression vector of CM_{Cg}M1: deletion of residues 98–100	This study
pET28-CM_{Cg}M2	Expression vector of CM_{Cg}M2: deletion of residues 97–101	This study
pET28-CM_{Cg}M3	Expression vector of CM_{Cg}M3: residues ^{60}SGGTR^{64} are mutated to ^{60}AAAAA^{64}	This study
pET28-CM_{Cg}M4	Expression vector of CM_{Cg} mutant: $R^{46}A$, $R^{57}A$	This study
pET21a	Expression vector with no tag	Novagen
pET21-DS_{Cg}	pET28a derivative for expression of DS_{Cg}	This study
pET21-DS_{Cg}M1	Expression vector of DS_{Cg}M1: residues ^{212}SPAGARYE^{219} are mutated to be ^{212}AAAAAAAAA^{219}	This study
pET21-DS_{Cg}M2	Expression vector of DS_{Cg}M2: residues ^{387}HFDKVIDE^{394} are mutated to be ^{387}AAAAAAAA^{394}	This study
Primer		
CM_{Cg}Fr	GACCATATGACTAATGCAGGTGAC	This study
CM_{Cg}M1Rr	CGAATTCTTATCCGCGTCCCATGCGCAGG	This study
CM_{Cg}M2Rr	CGAATTCTTATCCCATGCGCAGC	This study
CM_{Cg}M3Fr	CGCATGAGCGCGGCCGCAGCAGCTCTCGTGCACACCCGAGAAG	This study
CM_{Cg}M3Rr	GTGCACGAGAGCTGCTGCGGCCGCGCTCATGCGTGTTTTTCCGATG	This study
CM_{Cg}M4Fr1-1	GGTGAAACGCGCCACGAAGATTTCCCAAACCATC	This study
CM_{Cg}M4Rr2-1	GAAATCTTCGTGGCGCGTTTCACCGCATCGAGG	This study
CM_{Cg}M4Fr1-2	CATCGGAAAAACAGCCATGAGCTCGGGCGGAAC	This study
CM_{Cg}M4Rr2-2	CGAGCTCATGGCTGTTTTTCCGATGGTTTGGG	This study
DS_{Cg}Fr	CTCTAGAAAAGGAGGACATATGAATAGGGGTGTGAGTTGG	This study
DS_{Cg}Rr	GTGGATCCTGTGGAGCGGAGTTATCTTGA	This study
DS_{Cg}M1Fr	GAACCGCGAGTTCGTTGCGAACGCCGCAGCTGCTGCAGCCGCCGCGGCTCTTGCTCGTGAGATCGAC	This study
DSCgM1Rr	CGAGCAAGAGCCGCGGCGGCTGCAGCAGCTGCGGCGTTCGCAACG	This study
DSCgM2Fr	CATCCAATGGCTACAAGACCCGTGCCGCAGCTGCTGCAGCCGCCGCGGTCCAGGGCTTCTTCGAGGTC	This study
DSCgM2Rr	GCCCTGGACCGCGGCGGCTGCAGCAGCTGCGGCACGGGTCTTG	This study

Recombinant DS proteins in *E. coli* BL21 (DE3) cells were synthesized similarly but at 16 °C. Cells were harvested by centrifugation at 10,000×*g*, washed twice with 0.2 % KCl solution, resuspended in 50 mM Tris–HCl buffer (pH7.5), and disrupted by sonication in an ice-water bath. The cellular lysate was centrifuged at 20,000×*g* for 30 min at 4 °C, and the supernatant was used for protein purification.

Recombinant wild type and mutant CM_{Cg} proteins were purified with a His-Bind protein purification kit (Novagen, Madison, WI) according to the manufacturer's instructions. Wild-type DS_{Cg} and mutant DS_{Cg}M1 were purified by ammonium sulfate fractionation and chromatography on a HiTrap Q HP column (GE Healthcare, Little Chalfont, UK). The wild-type DS_{Cg} was recovered from ammonium sulfate solution at 20–35 % saturation. DS_{Cg}M1 was recovered from ammonium sulfate solution at 30–50 % saturation. Wild-type DS_{Cg} and mutant DS_{Cg}M1 crude extracts were individually loaded onto a HiTrap Q HP column. Both DS_{Cg} and DS_{Cg}M1 were eluted at NaCl concentrations ranging from 500–700 mM. Proteins were stored at −20 °C following concentration.

Chorismate mutase activity

CM activity was assayed by means of the procedure of Davidson and Hudson (1987). The assay mixture contained 50 mM Tris–HCl buffer (pH7.5, containing 1 mM dithiothreitol) and 1 mM chorismic acid in a total volume of 0.2 ml. After the mixture was incubated at 37 °C for 5 min, enzyme was added to initiate the reaction, and 10 min later, the reaction was stopped by the addition of 0.4 ml of 1 M HCl. One unit of CM activity was defined as the amount of enzyme that catalyzed the conversion of 1 μmol of chorismate to prephenate per minute under the conditions used. For calculations, we used $17.5\times10^{3}M^{-1}\times cm^{-1}$ as the extinction coefficient at 320 nm (ε_{320nm}) for phenylpyruvate (Davidson and Hudson 1987).

DS activity

DS activity was determined according to the procedure described by Siehl (1997). The assay mixture contained 50 mM Tris–HCl buffer (pH7.5), 5 mM PEP, 2 mM erythrose-4-phosphate, and enzyme in a volume of 75 μl. The mixture was incubated at 30 °C for 10 min. The reaction was initiated by the addition of enzyme and terminated by the addition of 400 μl of 10 % (wt/vol) trichloroacetic acid. Reaction mixtures without enzyme were run in parallel and used as controls. One unit of activity was defined as the amount of enzyme that catalyzed the synthesis of 1 μmol of DAHP per minute at 30 °C. For calculations, we used $4.5\times10^{4}M^{-1}\times cm^{-1}$ as the extinction coefficient for DAHP at 549 nm (ε_{549nm}) (Schoner and Herrmann 1976).

Inhibition of DS activity by prephenate was determined by inclusion of prephenate in the assay mixtures. Parallel experiments without enzyme in the assay mixture were run as controls. Inhibition constants (K_i) were calculated by means of Dixon plots (Dixon 1953).

Measurements of protein concentrations

Protein concentrations were measured according to the method of Bradford (1976), with bovine serum albumin as the standard.

Results

Regulation of DS_{Cg} activity by prephenate in the presence of CM_{Cg} and identification of a putative prephenate binding site on CM_{Cg}

In this study, we observed that in the presence of CM_{Cg}, 2 mM prephenate inhibited DS_{Cg} activity by 45.6 %. The K_i

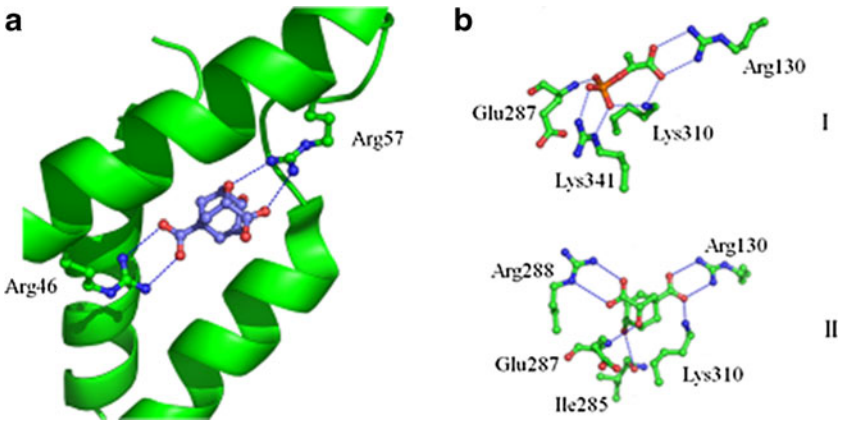

Fig. 1 Prediction of chorismate/prephenate binding sites in the putative DS_{Cg}-CM_{Cg} complex. (**a**) Key amino acid residues involved in the binding of prephenate to the complex. (**b**) Amino acid residues involved in the binding of PEP and prephenate to the complex. Prephenate was modeled in the PEP binding site of DS_{Cg} in the complex. (**I**) amino acid residues involved in the binding of PEP; (**II**) putative amino acid residues involved in the binding of prephenate. Hydrogen bonds are indicated with broken lines

Table 2 Specific activities of DS_{Cg} and CM_{Cg} and mutants. Values are averages from three parallel determinations and standard errors are provided

Enzyme or mutant	Specific activity (units/mg)
DAHP synthase activity	
DS_{Cg}	85.1±1.9
DS_{Cg}M1	56.4±3.0
DS_{Cg}M2	No activity
Chorismate mutase activity	
CM_{Cg}	124.0±6.9
CM_{Cg}M1	114.2±7.8
CM_{Cg}M2	112.7±12.4
CM_{Cg}M3	97.1±5.8
CM_{Cg}M4	No activity

value for prephenate was determined to be 0.945 mM. The inhibition by prephenate was competitive against PEP, but not against erythrose 4-phosphate.

Using the crystal structure of the DS_{Mt}-CM_{Mt} complex (Sasso et al. 2009), a binding site for analogs of chorismate and prephenate was observed. We further identified the corresponding amino acid residues in CM_{Cg} (Figs. 1a, b), and mutated two of the key amino acid residues, Arg^{46} and Arg^{57}. The resulting mutant, CM_{Cg}M4, showed no CM activity (Table 2), suggesting that Arg^{46} and Arg^{57} were essential for CM_{Cg} activity. To determine whether the inactive CM_{Cg}M4 interacted with DS_{Cg}, we investigated the effect of prephenate on DS activity in the presence of CM_{Cg}M4, and found that the regulatory effect was retained but was somewhat reduced (Table 3). Prephenate reduced DS activity by 26.6 % in the presence of mutant CM_{Cg}M4, whereas DS activity was reduced by 45.6 % in the presence of the wild-type CM_{Cg}.

Reexamination of the DS_{Mt}-CM_{Mt} structure and exploration of the interaction surfaces between DS_{Cg} and CM_{Cg}

The structures of DS_{Mt} and CM_{Mt} have previously been solved (PDB: 2B7O; PDB: 2QBV) (Kim et al. 2006; Webby et al. 2005). DS_{Mt} contains a core $(\beta/\alpha)_8$ triosephosphate isomerase barrel domain and CM_{Mt} consists of three α-helices. Recently, the structure of the DS_{Mt}-CM_{Mt} complex (PDB: 2W1A) also became available (Sasso et al. 2009). In this study, we reexamined these structures in an attempt to show the interaction interface between DS_{Mt} and CM_{Mt}. Sasso et al. (2009) reported that the DS_{Mt}-CM_{Mt} complex is composed of a central core of four DS_{Mt} subunits sandwiched between two CM_{Mt} dimers. Our examination of the DS_{Mt}-CM_{Mt} complex structure showed that two regions, designated I and II, play a key role in the interaction between DS_{Mt} and CM_{Mt} (Fig. 2a). Region I consists of two α-helices (α7, ^{383}HFDRIVDEVQGFFEVHRAL^{401}; α8, ^{445}NTQQSLELAFLVAEMLRD^{462}) of DS_{Mt} and the ^{64}SGGTR^{68} loop and C-terminus (^{100}RGRLG^{104}) of CM_{Mt}. Region II contains the ^{208}SPAGARYE^{215} loop between α2a and α2b of DS_{Mt} and H2 (^{71}HSREMKVIE^{79}) and H3 (^{89}KDLAILLLR^{97}) of CM_{Mt} (Fig. 2b).

DS_{Cg} and CM_{Cg} showed 77 and 57 % sequence identity to DS_{Mt} and CM_{Mt}, respectively. Therefore, we used the structure of DS_{Mt}-CM_{Mt} as a reference to identify the amino acid residues that mediate the interaction between DS_{Cg} and CM_{Cg}. The sequences of DS_{Cg} and CM_{Cg} were aligned with those of DS_{Mt} and CM_{Mt}, respectively (Fig. 2b). Residues in the ^{60}SGGTR^{64} and ^{97}RGKLG^{101} regions of CM_{Cg} and the ^{212}SPAGARYE^{219} and ^{387}HFDKVIDE^{394} regions of DS_{Cg} corresponded to residues in the ^{64}SGGTR^{68} (orange) and ^{100}RGRLG^{104} (magenta) regions of CM_{Mt} and to residues in the ^{208}SPAGARYE^{215} (blue) and ^{383}HFDRIVDE^{390} (red) regions of DS_{Mt} (Fig. 2a), respectively. We deduced that

Table 3 Effects of prephenate (2 mM) on DS_{Cg} and DS_{Cg}M1 activities when CM_{Cg} or CM_{Cg} mutants were present in the reaction mixtures. Values are averages from three parallel determinations and standard errors are provided

Enzyme assays	Remained DS activity (%)	Specific DS activity (units/mg)
DS_{Cg}+CM_{Cg}	100.0±5.8	95.3±5.5
DS_{Cg}+CM_{Cg}+prephenate	54.4±6.3	51.8±6.0
DS_{Cg}+CM_{Cg}M1	100±2.3	93.0±2.1
DS_{Cg}+CM_{Cg}M1+prephenate	86.8±3.3	80.7±3.1
DS_{Cg}+CM_{Cg}M2	100±15.1	87.3±13.2
DS_{Cg}+CM_{Cg}M2+prephenate	84.8±16.2	74.0±14.1
DS_{Cg}+CM_{Cg}M3	100±7.7	81.7±6.2
DS_{Cg}+CM_{Cg}M3+prephenate	70.8±8.3	57.8±6.8
DS_{Cg}+CM_{Cg}M4	100±5.6	70.3±3.9
DS_{Cg}+CM_{Cg}M4+prephenate	73.4±11.0	51.6±7.7
DS_{Cg}M1+CM_{Cg}	100±6.0	58.2±3.5
DS_{Cg}M1+CM_{Cg}+prephenate	89.6±15.8	52.1±9.2

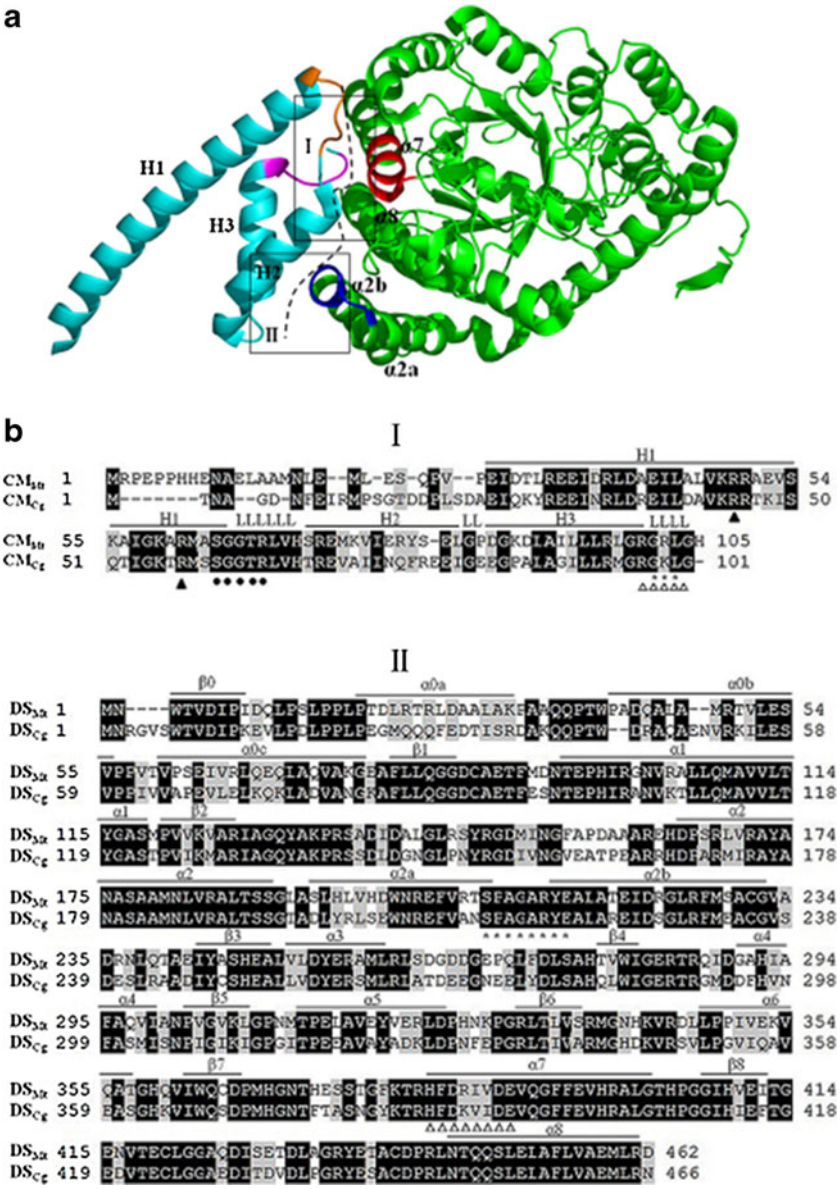

Fig. 2 (**a**) Structure modeling of DS_{Mt}-CM_{Mt} interface regions: (*cyan*) CM_{Mt} monomer, (*green*) DS_{Mt} monomer, (*H1, H2, and H3*) α-helices of CM_{Mt}. Mutated sites (*orange, magenta, red, and blue*). (**b**) Identification of corresponding regions of the interaction interface of the DS_{Cg}-CM_{Cg} complex by sequence alignment: (*H*) α-helix, (*L*) loop; (*) CM_{Cg}M1 or DS_{Cg}M1, (△) CM_{Cg}M2 or DS_{Cg}M2, (●) CM_{Cg}M3, and (▲) CM_{Cg}M4

these amino acid residues were involved in the interaction between DS_{Cg} and CM_{Cg}, and therefore, we subjected them to mutagenesis analysis.

Construction of DS_{Cg} and CM_{Cg} mutants and determination of their catalytic activities

We constructed two DS_{Cg} mutants [DS_{Cg}M1 (^{212}SPAGARYE^{219}) and DS_{Cg}M2 (^{387}HFDKVIDE^{394})] and three CM_{Cg} mutants [CM_{Cg}M1 (^{98}GRL^{100}), CM_{Cg}M2 (^{97}RGRLG^{101}), and CM_{Cg}M3 (^{60}SGGTR^{64})] by replacing or deleting the amino acid residues indicated in parentheses. Upon induction with isopropyl ß-D-1-thiogalactopyranoside, recombinant *E. coli* BL21 (DE3) cells promptly synthesized the target proteins. All target proteins were obtained as soluble proteins, except DS_{Cg}M2, which was

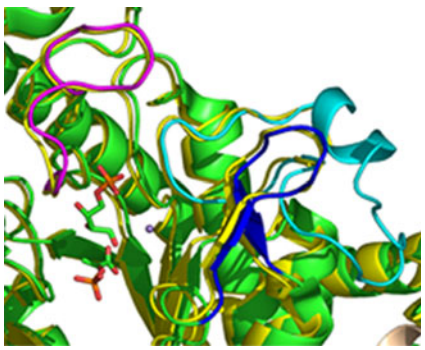

Fig. 3 Models of the structures of DS_{Cg} and the DS_{Cg}-CM_{Cg} complex: (*yellow*) DS_{Cg}, (*green*) DS_{Cg} in the DS_{Cg}-CM_{Cg} complex, and (*magenta, blue, and cyan*) three loops above the DS_{Cg} catalytic center discussed in the text. These models were based on the structures of DS_{Mt} (PDB: 2B7O) and the DS_{Mt}-CM_{Mt} complex (PDB: 2W1A)

obtained as insoluble inclusion bodies and showed no activity. The proteins were purified from recombinant *E. coli* BL21 (DE3) cells, and their catalytic activities were determined. Enzymatic activity assays demonstrated that the activities of all the CM_{Cg} mutants were nearly identical to the original activities, indicating that the mutated amino acid residues were not essential for activity.

Effect of site-directed mutagenesis on prephenate regulation of DS activity

To explore the DS_{Cg} and CM_{Cg} interaction and the regulation of DS_{Cg} by prephenate, we determined DS activities with wild-type DS_{Cg} and mutants of CM_{Cg}, as well with mutant DS_{Cg} and wild-type CM_{Cg} (Table 3). The regulatory effect of prephenate on DS_{Cg} activity in the presence of CM_{Cg}M1 or CM_{Cg}M2 was significantly reduced compared with the effect in the presence of CM_{Cg}: DS_{Cg} activity was reduced by 13.2 and 15.2 % in the presence of CM_{Cg}M1 or CM_{Cg}M2, respectively. The regulatory effect of prephenate in the presence of CM_{Cg}M3 remained strong (prephenate reduced DS_{Cg} activity by 29.2 %). Regulation of DS activity by prephenate was retained in the DS_{Cg}M1-CM_{Cg} complex, but to a lesser extent than in the DS_{Cg}-CM_{Cg} complex (Table 3). Both CM_{Cg}M1 and CM_{Cg}M2 have a truncated C-terminus, whereas CM_{Cg}M3 carries a deletion far from the C-terminus. In consideration of the results described in this and previous sections, we concluded that the C-terminus of CM_{Cg} was important for the CM_{Cg} and DS_{Cg} interaction.

Discussion

C. glutamicum is a commercial important amino acid producer and plays a key role in the production of glutamate, lysine, and various vitamins (Ikeda and Nakagawa 2003). In this study, we examined the interaction between CM_{Cg} and DS_{Cg} with bioinformatic tools and experimental confirmation. Taken together, these results suggest that disruption of the amino acid residues of either DS_{Cg} or CM_{Cg} at the interaction interface of the putative DS_{Cg}-CM_{Cg} complex affected the interaction between the two proteins and thus altered the regulatory effect of prephenate on the DS activity of the DS_{Cg}-CM_{Cg} complex. We concluded that prephenate regulation of DS_{Cg} activity interactions relied on the interaction surfaces between DS_{Cg} and CM_{Cg} molecules. However, additional mechanism for prephenate regulation of DS_{Cg} activity might exist. As indicated by our results, prephenate competed for PEP in the presence of CM_{Cg} but not in DS_{Cg} alone. Considering that PEP is one of the substrates for DAHP synthase, it would be interesting to explore further that CM_{Cg} also had binding site for prephenate and/or PEP. To elucidate why prephenate was able to compete with PEP for the binding site in the DS_{Cg}-CM_{Cg} complex, we modeled the putative DS_{Cg}-CM_{Cg} complex and DS_{Cg} structures using structural information for the DS_{Mt}-CM_{Mt} complex and DS_{Mt} alone (Sasso et al. 2009; Webby et al. 2005). The model suggested that prephenate binds at the binding site of PEP in the catalytic center of DS_{Cg}. Further analysis revealed that three loops, ^{138}PRSSDLDGNGLPN^{150} (magenta), ^{375}NTFTASNG YKTR^{386} (blue), and ^{418}G(AA)$_{27}$P^{446} (cyan), were located near the catalytic center of DS_{Cg} (Fig. 3). Comparison of the structural models for DS_{Cg} and the DS_{Cg}-CM_{Cg} complex revealed that the ^{418}G(AA)$_{27}$P^{446} loop in DS_{Cg} was flexible, as previously reported for DS_{Mt} by Webby et al. (2005), whereas in the complex, the loop was rigid owing to its interaction with CM_{Cg}. We hypothesized that the flexible ^{418}G(AA)$_{27}$P^{446} loop prevented the entrance of prephenate into the catalytic center of DS_{Cg}. This hypothesis would explain why prephenate inhibited DS_{Cg} activity by competing for PEP in the presence of CM_{Cg} but not in its absence. Our hypothesis is supported by a report that conformational changes in amino acid loops near the catalytic center of the DS in *Thermotoga maritima* regulate the enzyme's activity (Shumilin et al. 2004). The new knowledge on the regulation of DS activity from this study might be useful for the construction of more productive strains of aromatic amino acids with *C. glutamicum*.

Acknowledgments This work was supported by a grant from the Ministry of Science and Technology of China (973-project, grant no. 2012CB721104).

References

Bradford MM (1976) A rapid and sensitive method for the quantization of microgram quantities of protein utilizing the principle of protein-dye binding. Anal Biochem 72:248–254

Davidson BE, Hudson GS (1987) Chorismate mutase-prephenate dehydrogenase from *Escherichia coli*. Methods Enzymol 142:440–450

DeLano WL (2002) Unraveling hot spots in binding interfaces: progress and challenges. Curr Opin Struct Biol 12:14–20

Dixon M (1953) The determination of enzyme inhibitor constants. Biochem J 55:170–171

Herrmann KM (1995) The shikimate pathway: early steps in the biosynthesis of aromatic compounds. Plant Cell 7:907–919

Ikeda M, Nakagawa S (2003) The *Corynebacterium glutamicum* genome: features and impacts on biotechnological processes. Appl Microbiol Biotechnol 62:99–109

Jiao W, Hutton RD, Cross PJ, Jameson GB, Parker EJ (2012) Dynamic cross-talk among remote binding sites: the molecular basis for unusual synergistic allostery. J Mol Biol 415:716–726

Kikuchi Y, Tsujimoto K, Kurahashi O (1997) Mutational analysis of the feedback sites of phenylalanine-sensitive 3-deoxy-D-arabino-heptulosonate-7-phosphate synthase of *Escherichia coli*. Appl Environ Microbiol 63:761–762

Kim SK, Reddy SK, Nelson BC, Vasquez GB, Davis A, Howard AJ, Patterson S, Gilliland GL, Ladner JE, Reddy PT (2006) Biochemical and structural characterization of the secreted chorismate mutase (Rv1885c) from *Mycobacterium tuberculosis* H37Rv: an *AroQ enzyme not regulated by the aromatic amino acids. J Bacteriol 188:8638–8648

Li PP, Liu YJ, Liu SJ (2009) Genetic and biochemical identification of the chorismate mutase from *Corynebacterium glutamicum*. Microbiology 155:3382–3391

Liao HF, Lin LL, Chien HR, Hsu WH (2001) Serine 187 is a crucial residue for allosteric regulation of *Corynebacterium glutamicum* 3-deoxy-D-arabino-heptulosonate 7-phosphate synthase. FEMS Microbiol Lett 194:59–64

Liu YJ, Li PP, Zhao KX, Wang BJ, Jiang CY, Drake HL, Liu SJ (2008) *Corynebacterium glutamicum* contains 3-deoxy-D-arabino-heptulosonate 7-phosphate synthases that display novel biochemical features. Appl Environ Microbiol 74:5497–5503

Pittard AJ (1996) Biosynthesis of aromatic amino acids in *Escherichia coli* and *Salmonella*. Cellular and Molecular Biology. American Society of Microbiology, Washington, pp 458–484

Romero RM, Roberts MF, Phillipson JD (1995) Anthranilate synthase in microorganisms and plants. Phytochemistry 39:263–276

Samsbrook J, Fritsch EF, Maniatis T (1989) Molecular cloning: a laboratory manual, 2nd edn. Cold Spring Harbor Laboratory Press, New York

Sasso S, Okvist M, Roderer K, Gamper M, Codoni G, Krengel U, Kast P (2009) Structure and function of a complex between chorismate mutase and DAHP synthase: efficiency boost for the junior partner. EMBO J 28:2128–2142

Schneider CZ, Parish T, Basso LA, Santos DS (2008) The two chorismate mutases from both *Mycobacterium tuberculosis* and *Mycobacterium smegmatis*: biochemical analysis and limited regulation of promoter activity by aromatic amino acids. J Bacteriol 190:122–134

Schoner R, Herrmann KM (1976) 3-Deoxy-D-arabino-heptulosonate 7-phosphate synthase. Purification, properties, and kinetics of the tyrosine-sensitive isoenzyme from *Escherichia coli*. J Biol Chem 251:5440–5447

Siehl DL (1997) Inhibitors of EPSP synthase, glutamine synthetase, and histidine synthesis. In: Row RM, Burton JD, Kuhr RJ (eds) Herbicide Activity: Toxicology, Biochemistry and Molecular Biology. IOS Press, Amsterdam, pp 37–67

Shumilin IA, Bauerle R, Wu J, Woodard RW, Kretsinger RH (2004) Crystal structure of the reaction complex of 3-deoxy-D-arabino-heptulosonate-7-phosphate synthase from *Thermotoga maritima* refines the catalytic mechanism and indicates a new mechanism of allosteric regulation. J Mol Biol 341:455–466

Tauch A, Kassing F, Kalinowski J, Pühler A (1995) The *Corynebacterium xerosis* composite transposon Tn5432 consists of two identical insertion sequences, designated IS1249, flanking the erythromycin resistance gene ermCX. Plasmid 34:119–131

Tauch A, Kirchner O, Loffler B, Gotker S, Pühler A, Kalinowski J (2002) Efficient electrotransformation of *Corynebacterium diphtheriae* with a mini-replicon derived from the *Corynebacterium glutamicum* plasmid pGA1. Curr Microbiol 45:362–367

Thompson JD, Gibson TJ, Plewniak F, Jeanmougin F, Higgins DG (1997) The CLUSTAL_X windows interface: flexible strategies for multiple sequence alignment aided by quality analysis tools. Nucleic Acids Res 25:4876–4882

Wang RH, Chen RC, Liu RZ (2008) A modified method of QuikChange site-directed mutagenesis. J Xiamen Univ 47:z2

Webby CJ, Baker HM, Lott JS, Baker EN, Parker EJ (2005) The structure of 3-deoxy-D-arabino-heptulosonate 7-phosphate synthase from *Mycobacterium tuberculosis* reveals a common catalytic scaffold and ancestry for type I and type II enzymes. J Mol Biol 354:927–939

Webby CJ, Jiao W, Hutton RD, Blackmore NJ, Baker HM, Baker EN, Jameson GB, Parker EJ (2010) Synergistic allostery, a sophisticated regulatory network for the control of aromatic amino acid biosynthesis in *Mycobacterium tuberculosis*. J Biol Chem 285:30567–30576

Wu J, Sheflyan GY, Woodard RW (2005) *Bacillus subtilis* 3-deoxy-D-arabino-heptulosonate 7-phosphate synthase revisited: resolution of two long-standing enigmas. Biochem J 390:583–590